# Pathogen Clearance-based Correlates of Immunoprotection Reveal Insightful Features of Vaccine Immunity

Xianbin Tian[1], Juanjuan Wang[1,2]*, Haoze Chen[1], Ming Ding[1], Qian Jin[1], and Jing-Ren Zhang[1,2]*

[1]Center for Infectious Disease Research, Department of Basic Medical Science, School of Medicine, Tsinghua University, Beijing, China;

[2]Tsinghua-Peking Center for Life Sciences, Tsinghua University, Beijing, China;

***Correspondence** to: wangjj15@tsinghua.org.cn or zhanglab@tsinghua.edu.cn

## ABSTRACT

Vaccination has significantly reduced the incidence of invasive infections caused by several bacterial pathogens, including *Streptococcus pneumoniae, Haemophilus influenzae* and *Neisseria meningitidis*. However, no vaccines are available for many other invasive pathogens. A major hurdle in vaccine development is the lack of functional markers to quantify vaccine immunity in eliminating pathogens in the process of infection. Based on our recent discovery of the liver as the major organ of vaccine-induced clearance of blood-borne virulent bacteria, we here describe a new vaccine evaluation system that quantitatively characterize important properties of effective vaccines in shuffling virulent bacteria from the blood circulation to the liver resident macrophage Kupffer cells (KCs) and sinusoidal endothelial cells (LSECs) in animal models. This system consists of three related correlates or assays: pathogen clearance from the bloodstream, pathogen trapping in the liver, and pathogen capture by KCs/LSECs. The readouts of these correlates were consistently associated with the serotype-specific immunoprotection levels of the 13-valent pneumococcal polysaccharide conjugate vaccine (PCV13) against lethal infections of *S. pneumoniae,* a major invasive pathogen of community-acquired infections in humans. Furthermore, these assays were able to identify a set of functional differences between two licensed PCV13 brands. Finally, the reliability and sensitivity of these correlates in reflecting vaccine efficacy were verified with whole cell vaccines of *Klebsiella pneumoniae* and *Escherichia coli*, two major pathogens in hospital-acquired invasive infections. This system may be used as cost effective readouts to evaluate the immunoprotective potential of vaccine candidates in the preclinical phase by filling the current technical gap in vaccine evaluation between the conventional *in vitro* approaches (e.g., antibody production and pathogen neutralization/opsonophagocytosis) and survival of immunized animals.



**Key words:** vaccine, immunoprotection, blood infection, *Streptococcus pneumoniae*, liver, Kupffer cell, and liver sinusoidal endothelial cell.

## INTRODUCTION

Sepsis caused by microbial infections of the blood circulation represents an important global health problem and economic burden[1,2]. Approximately 49 million sepsis cases and 11 million sepsis-associated deaths were reported worldwide in 2017, representing 19.7% of all global deaths[2]. Sepsis pathogenesis is initiated by the entry and proliferation of microbial pathogens in the blood circulation, subsequent induction of excessive inflammatory responses, and life-threatening multi-organ dysfunctions[3]. Pathogenic bacteria are the common pathogens of septic infections, which consist of both the Gram-positive bacteria (*Streptococcus pneumoniae*, *Staphylococcus aureus*, *Staphylococcus epidermidis*, and *Enterococcus faecalis*) and Gram-negative bacteria (*Acinetobacter baumannii*, *Escherichia coli*, *Klebsiella pneumoniae*, and *Pseudomonas aeruginosa*)[4].

*S. pneumoniae* (pneumococcus), an encapsulated Gram-positive bacterium residing in the nasopharynx of humans, is an opportunistic pathogen of community-acquired pneumonia, bacteremia, and meningitis, particularly in children under 5 years old and the elderly[5]. There are forms of capsular polysaccharide (CPS)-based vaccines globally licensed to prevent invasive pneumococcal diseases (IPDs) (e.g. bacteremia and meningitis): pneumococcal polysaccharide vaccine (PPV) and pneumococcal conjugate vaccine (PCV)[6]. PPV is the first generation of pneumococcal vaccine that contains T cell-independent CPS antigens with poor immunogenicity in children under two years of ages[7]. PCV represents the next generation of CPS-based vaccine, in which CPSs are chemically linked to carrier proteins (e.g. diphtheria and tetanus toxoids) to activate both B and T lymphocytes to produce IgG antibodies[8]. The global recommendation of PCV has significantly reduced the pneumococcus-associated death worldwide[9]. Since the first introduction of PCV7 (Prevnar by Wyeth) that contains the CPSs of 7 IPD-associated serotypes, several PCVs with additional serotypes have been introduced, such as PCV10 (Synflorix by GlaxoSmithKline), PCV13 (Prevnar 13 by Pfizer, Weuphoria by Walvax, Weiminfeibao by Minhai), PCV15 (Vaxneuvance by Merck), PCV20 (Prevnar 20 by Pfizer)[6,10]. The three abovementioned PCV13 brands are all licensed in China.

Vaccination has greatly contributed to the control of many infectious diseases. While programmed immunization has led to global eradication (e.g., smallpox) or nearly eradication (e.g., polio) of a few viral diseases, a number of bacterial diseases have become preventable by vaccination, such as diphtheria (*Corynebacterium diphtheria*), whooping cough (*Bordetella pertussis*), tetanus (*Clostridium tetani*), meningitis (*Neisseria meningitidis*), bacterial pneumonia and sepsis (*S. pneumoniae*, *Haemophilus influenzae*). Except for *S. pneumoniae*, there are no available vaccines for any of the major blood infection pathogens after many

unsuccessful efforts in developing vaccines for each of these pathogens. One of the major hurdles in the process of the current vaccine development is the lack of reliable and sensitive immunoprotection correlates to identify any problems in the early steps of vaccine development. Protection efficacy of vaccines relies on two functional aspects of immunization: 1) the features of vaccine-induced antibody and/or T-cell responses, and 2) the potency of vaccine-elicited immunity of pathogen elimination upon pathogen entry[11]. Beyond protection against infections in animal models (e.g., survival rate), the current vaccine evaluation system mostly depends on *in vitro* assessment of vaccine-induced immune responses, such as antibody titer, antibody-mediated neutralization and opsonophagocytosis of pathogen. As an example, the current pneumococcal vaccines are based on measuring antibody level by enzyme-linked immunosorbent assay (ELISA) and antibody-mediated phagocytosis of neutrophil by opsonophagocytic killing assay (OPKA)[12,13]. These parameters don't inform how vaccine-elicited immunity enable hosts to recognize and clear pathogens in the process of infection. Therefore, there is a great need for reliable and sensitive *in vivo* techniques for functional evaluation of vaccine immunity in the recognition and elimination of invading pathogens in the process of infection.

The liver represents a major organ to capture and eliminate invading microbes from the blood circulation, which are executed by the liver resident macrophage Kupffer cells (KCs) and liver sinusoidal endothelial cells (LSECs)[14]. KCs and LSECs represent approximately 20% and 50% of the liver non-parenchymal cells (NPCs), respectively[15]. KCs are the most dominant resident macrophages in mammals, representing approximately 90% of total resident macrophages in the body[16]. While KCs are specialized for the clearance of large particles (e.g. bacteria)[17], LSECs preferentially clear small particles (e.g. viruses)[18]. Our recent studies have discovered that the liver is the major immune organ to execute vaccine-activated capture and killing of pathogenic bacteria in the bloodstream of mice[19,20]. In particular, PCV13 activates both KCs and LSECs to rapidly recognize and capture IgG-coated pneumococci in the bloodstream[20].

This study aims to establish an *in vivo* vaccine evaluation system to quantify the functional features of vaccine-activated pathogen clearance from the blood circulation to the liver, based on our recent findings of liver-based vaccine immunity[19,20]. We have developed three related new correlates or assays: pathogen clearance from the bloodstream, pathogen trapping in the liver, and pathogen capture by KCs/LSECs in the liver sinusoids. The reliability and sensitivity of these assays have been tested in three pathogens and four vaccines. Potential applications of this new system in vaccine evaluation and development are discussed.

## RESULTS

### The clearance rate of blood-borne pneumococci predicts the protection efficacy of PCV13

Our recent studies have shown that effective clearance of bacteria from the bloodstream in the early phase of septic infections is essential for host survival[21], and efficient vaccination enhances such the pathogen clearance of certain encapsulated high-virulence bacteria that otherwise persist in the blood circulation[19,20]. To assess the direct relationship between the vaccine-elicited pathogen clearance rate and host survival, we compared the PCV13-induced bacterial clearance of different vaccine-covered serotypes of pneumococci from the bloodstream. In particular, we focused on the five high-virulence (HV) serotypes (1, 3, 4, 5 and 6A) covered by PCV13 because the clearance of these serotypes highly depends on PCV13 immunization in mice[19,20], and the rest of the eight low-virulence (LV) serotypes (6B, 7F, 9V, 14, 18C, 19A, 19F and 23F) are effectively cleared in naïve mice[21]. We first measured CPS-specific IgG antibodies in PCV13-immunized and control mice by enzyme-linked immunosorbent assay (ELISA) because antibody titer has been used as an efficacy marker of pneumococcal polysaccharide conjugate vaccines[22,23]. Though PCV13 immunization generated antibodies to each of the five serotypes, the ELISA results revealed substantial variations in antibody level, with serotypes 4 and 6A as the highest and lowest in the antibody range, respectively (**Fig. 1A**). We next monitored the dynamic of bacteremia in immunized and control mice during the first 30 min post intravenous (i.v.) infection of pneumococci. In the adjuvant group, all of the five representative strains retained abundantly in blood circulation within 30 min post i.v. infection of $10^6$ CFU (**Fig. 1B**). In contrast, the circulating pneumococci were cleared quickly from the bloodstream even to undetectable level in PCV13-immunized mice at 30 min post infection (**Fig. 1C**). Consistent with our previous findings of serotype-3 and -4 pneumococci[20], this result demonstrates that PCV13 induces fast pneumococcal clearance of all the five HV serotypes from the bloodstream.

Previous studies have indicated that pneumococcal conjugate vaccines PCV7/PCV13 confer relatively poor protection against invasive disease caused by serotype 3 in humans[24-26]. We next tested if pathogen clearance rate could identify this functional difference in mice using higher challenge doses. PCV13-immunized mice rapidly cleared $10^7$ CFU of serotype-4, -5 and -6A pneumococci from the circulation with $CT_{50}$ of 1.5, 0.7, and 0.8 min, respectively. In sharp contrast, serotype-1 and -3 pneumococci were still largely circulating in the blood of the immunized mice with marginal reduction in bacteremia level post i.v. inoculation with $10^7$ CFU (**Fig. 1D**). With a much higher infection dose ($10^8$ CFU), the immunized mice still rapidly cleared 99% inoculum of serotype-5 and -4 pneumococci with $CT_{50}$ of 0.7 and 1.5 min,

respectively (**Fig. 1E**), but were incapable of effectively clearing the other 3 serotypes at this infection dose, with 58%, 74%, and 32% of serotype-1, -3 and -6A inoculum being still detected in the circulation at 30 min, respectively. Overall, these experiments have ranked the functional capacity of PCV13 immunization in clearing the five HV serotypes in the following order: 5, 4, 6A, 1 and 3. The uneven clearance of various serotypes in PCV13-immunized mice strongly suggests that the different antigens in PCV13 elicit variable levels of functional immunity.

To determine if the differences of PCV13-elicited clearance of various pneumococcal serotypes reflect protection efficacy against different serotypes of *S. pneumoniae*, we measured the survival of PCV13-immunized mice post intraperitoneal (i.p.) infection. Compared with the full mortality of adjuvant groups post i.p. infection with $10^6$ CFU, PCV13-immunized mice conferred a full protection against serotype 1 (**Fig. 1F**), 4 (**Fig. 1H**), 5 (**Fig. 1I**) and 6A (**Fig. 1J**), and 80% protection against serotype 3 (**Fig. 1G**). We further determined the upper limits of PCV13 immunization against each serotype with higher levels of inoculum. In line with the different impacts of PCV13 on blood clearance of the five serotypes (**Figs. 1D-E**), the vaccination conferred the strongest protection against lethal infection of serotype-4, -5 and -6A pneumococci, with a 50% lethal dose ($LD_{50}$) of $7.1 \times 10^7$ CFU (**Fig. 1H**), $1.2 \times 10^8$ CFU (**Fig. 1I**) and $5.6 \times 10^7$ CFU (**Fig. 1J**), respectively. By comparison, the immunized mice were much more susceptible to infection of serotype-3 pneumococci with a $LD_{50}$ of $2.2 \times 10^6$ CFU (**Fig. 1G**), and, to a less extent, to that of serotype-1 pneumococci ($LD_{50} = 3.2 \times 10^7$ CFU) (**Fig. 1F**). Overall comparison revealed a dramatic 54.5-fold difference in $LD_{50}$ between the best (serotype 5) and worst (serotype 3) protected categories. The order of protection efficacy induced by PCV13 immunization against infection of the HV serotypes (5, 4, 6A, 1 and 3) is the same as the order of blood pathogen clearance rate. Taken together, these results demonstrate that the PCV13-elicited pathogen clearance rate in the bloodstream is highly predictive of the protection efficacy.

**Hepatic trapping of blood-borne pneumococci correlates the protection efficacy of PCV13**

Our recent studies have found that the liver is the major executive organ for vaccine-induced trapping of high-virulence encapsulated *S. pneumoniae*[20] and *Klebsiella pneumoniae* serotypes[19] from the blood circulation. To determine the potential of vaccine-activated hepatic pathogen trapping as a functional correlate for vaccine protection efficacy, we detected the bacterial CFU count in five major organs and blood as previously described[20]. Consistent with the poor clearance of the five HV serotypes in mice of adjuvant group, these animals showed

174 marginal pathogen trapping in the liver for serotypes 1, 3, 4, 5, and 6A post i.v. infection with
175 $10^6$ CFU (**Fig. 2A**). In contrast, virtually all of the viable pneumococci in PCV13-immunized
176 mice were detected in the liver, with near sterilization of the blood circulation, at 30 min post
177 i.v. infection with $10^6$ CFU (**Fig. 2B**). Comparison of the total CFU counts between PCV13
178 and adjuvant groups revealed significantly lower levels of bacterial burden in vaccinated mice,
179 which reflected vaccine-activated pathogen killing in the liver[20], and the full protection of
180 vaccinated mice against infection with $10^6$ CFU of the five HV serotypes (**Fig. 1**). However,
181 PCV13-immunized mice displayed a serotype-specific pattern of vaccine-activated pathogen
182 trapping in the liver at higher levels of infection dose. Although the majority of viable serotype-
183 1 (77%), -3 (72%), -4 (84%), -5 (91%) and -6A (86%) pneumococci were still found in the
184 livers of PCV13-immunized mice at 30 min post i.v. infection with $10^7$ CFU, serotype-1 (18%)
185 and -3 (20%) pneumococci escaped hepatic capture and remained in the bloodstream (**Fig. 2C**).
186 The vaccine-induced hepatic trapping of the five serotypes is ranked from the highest to the
187 lowest as: 5, 6A, 4, 1 and 3. Relatively poorer hepatic trapping of serotypes 1 and 3 in the
188 immunized mice was also reflected by relatively higher levels of total bacteria detected for
189 these two serotypes at 30 min. When infection dose was increased to $10^8$ CFU, relative
190 proportion of hepatic pathogen trapping was in the order as: 5 (97%), 4 (96%), 6A (21%), 3
191 (19%) and 1 (3%) and serotype-specific variation in vaccine-induced hepatic pathogen trapping
192 became more dramatic (**Fig. 2D**). These results show that vaccine-activated hepatic trapping
193 of blood-borne pneumococci strongly correlates with the protection efficacy of PCV13.
194

195 **Pathogen capture by liver immune cells indicates the protection efficacy of PCV13**

196 The vaccine-activated dual-track bacterial capture by liver resident macrophages
197 Kupffer cells (KCs) and sinusoidal endothelial cells (LSECs) has been found as the cellular
198 basis of vaccine-elicited pathogen trapping in the liver[20,21]. To assess the potential of cellular
199 capture of circulating pathogens as a functional correlate for vaccine protection efficacy, time-
200 lapse intravital microscopy (IVM) imaging was used to visualize and quantify cellular capture
201 of serotype-1, -3, -4, -5 and -6A pneumococci post i.v. infection with $5 \times 10^7$ CFU in the liver
202 sinusoids of PCV13-immunized and control mice. While IVM showed that the HV
203 pneumococci were mostly passing the vasculature of control mice (**Fig. 3A, Movies 1-5, left**
204 **panel**), but were rapidly tethered mainly onto LSECs and less on KCs (**Fig. 3A, Movies 1-5,**
205 **right panel**). In agreement with the serotype-specific protection efficacies of PCV13 (**Fig. 1E**),
206 quantification of immobilized bacteria per field of view (FOV) revealed the highest numbers
207 of total captured bacteria for serotypes 4 (110) and 5 (87) as compared with fewer bacteria for

208 serotypes 1 (64), 3 (61) and 6A (74) (**Fig. 3B**). The real-time imaging of vaccine-activated
209 pathogen capture by the liver immune cells in live mice has provided immune cell-based data
210 that are consistent with the protection efficacy of PCV13.
211
212 **The *in vivo* immunoprotection correlates distinguish the potency levels of different**
213 **PCV13 brands**
214 The abovementioned data have established an *in vivo* system to evaluate vaccine protection
215 efficacy against bacterial septic infection, including the quantitation of pathogen clearance
216 from blood, trapping in the liver, and cellular capture by LSECs and KCs. Since these
217 parameters uncovered remarkable differences of PCV13-induced immunity in protecting lethal
218 infection against different vaccine-covered HV pneumococcal serotypes, we wondered
219 whether PCV13 vaccines have brand-specific differences in protecting against lethal infection
220 of the same serotypes of pneumococci, which could reveal potential differences of vaccine
221 efficacy. We thus compared abovementioned PCV13 (referred to as PCV13) with another brand
222 of PCV13 (referred to as PCV13X) using the three parameters, which are both licensed in
223 China. When i.v. challenged with $10^7$ CFU of bacteria, mice immunized by PCV13 showed
224 significant faster clearance of serotype-1 pneumococci ($CT_{50}$, 3.7 min) than the PCV13X-
225 immunized counterparts ($CT_{50}$, >30 min) (**Fig. 4A, left panel**). Accordingly, PCV13
226 immunization yielded more potent hepatic trapping as evidenced by the relative higher
227 proportion of liver-trapped bacteria out of the total viable bacteria in PCV13-immunized mice
228 (77%) than that in PCV13X-immunized counterparts (26%) (**Fig. 4A**, **middle panel**). Although
229 there was a modest difference in the total bacteria captured by the liver immune cells between
230 PCV13- and PCV13X-immunized mice, it is worth to mention that PCV13 induced a
231 significantly more potent bacterial capture by LSECs than PCV13X (**Fig. 4A**, **right panel,**
232 **Movie 6**), which may explain the difference in protection efficacy between the two vaccines
233 (**Fig. 5**). In a similar pattern, PCV13 immunization also yielded a more effective clearance of
234 serotype-3 pneumococci ($CT_{50}$, 7.1 min) than PCV13X ($CT_{50}$, >30 min), which is mirrored by
235 more effective hepatic trapping and cellular capture of the pathogen in PCV13-immunized
236 mice (**Figs. 4B** and **4F**, **Movie 7**). To a less extent, PCV13 also exhibited a similar pattern of
237 functional advantage over the other brand in the three aspects of pneumococcal clearance of
238 serotype 6A, with more efficient levels of blood pathogen clearance ($CT_{50}$ of 0.8 min for
239 PCV13 vs. 2.0 min for PCV13X), hepatic trapping (86% for PCV13 vs. 88% for PCV13X) and
240 total cellular capture in the liver sinusoids (74 for PCV13 vs. 47 for PCV13X) (**Figs. 4C** and
241 **4F**; **Movie 8**).

242 Potential brand-specific vaccine effects for serotype-4 and -5 pneumococci were evaluated
243 with an infection dose of $10^8$ CFU because this was the most revealing dose for the serotype-
244 specific vaccine effects of these two types (**Fig. 1**). While infection with serotype-4
245 pneumococci revealed no substantial differences between the two vaccines in the three
246 parameters (**Figs. 4D** and **4F**, **Movie 9**), PCV13 showed the most dramatic advantage over the
247 other brand in the vaccine effects against serotype-5 pneumococci. PCV13-immunized mice
248 displayed a highly efficient blood clearance ($CT_{50}$ of 0.7 min for PCV13 vs. >30 min for
249 PCV13X), hepatic trapping (97% for PCV13 vs. 15% for PCV13X) and total cellular capture
250 (87 for PCV13 vs. 36 for PCV13X) in the liver sinusoids (**Figs. 4E** and **4F**, **Movie 10**). Together,
251 these data show that the three *in vivo* immunoprotection correlates are capable of identifying
252 quantitative differences in vaccine-induced pathogen clearance functions.
253 We finally verified the PCV13 brand-specific variations in CPS-specific IgG antibodies
254 and protection against lethal infections. ELISA test revealed that PCV13 generally induced
255 more CPS-specific antibodies than PCV13X across the five serotypes tested thus far (**Fig. 5A**).
256 In a similar manner, PCV13 immunization led to a consistently more potent protection against
257 septic infections with all the five HV serotypes. With the doses that were fully protective by
258 PCV13, PCV13X immunization generated partial protection for serotype-1 (40%), -4 (60%),
259 and -5 (40%) pneumococci (**Figs. 5B, 5D** and **5E**). For the infection of both serotype-3 and -
260 6A pneumococci, PCV13 immunization conferred 80% protection of mice while PCV13X
261 immunization only provided 20% protection (**Figs. 5C** and **5F**). Overall, the superior protection
262 of PCV13 against septic infection of the HV pneumococcal serotypes than PCV13X agrees
263 with the quantitative differences of vaccine-activated pathogen clearance in the three novel *in*
264 *vivo* immunoprotection correlates. In summary, the novel *in vivo* vaccine evaluation system
265 with three immunoprotection correlates can accurately reveal the potency levels of
266 pneumococcal vaccines.
267
268 **The *in vivo* immunoprotection correlates reveal limited efficacy of whole cell vaccines**
269 We finally determined whether our PCV13-based *in vivo* vaccine evaluation system could
270 characterize the functional features of other vaccines beyond *S. pneumoniae.* This potential
271 was first tested with an inactivated whole cell vaccine (WCV) for a hypervirulent *Klebsiella*
272 *pneumoniae* (capsular serotype K2), a Gram-negative bacterium and a major pathogen of blood
273 infections in humans[27]. Our initial trial showed that the WCV confers a full protection against
274 lethal infection of the same *K. pneumoniae* strain (**Fig. 6A**). While all of naïve mice succumbed
275 to infection in the first 36 hr post i.p inoculation with $10^6$ CFU of bacteria, the group of

276 immunized mice completely survived the same challenge. Further analysis revealed that the
277 vaccinated mice gained the ability to clear *K. pneumoniae* from the blood circulation in the
278 first 30 min post i.v. inoculation, with a $CT_{50}$ of 0.6 min, whereas the pathogen were mostly
279 circulating in the bloodstream of naïve mice (**Fig. 6B**). Quantitation of bacteria in the liver and
280 other major organs uncovered 92% of detectable *K. pneumoniae* in the livers of vaccinated
281 mice as compared with 28% hepatic bacteria in naïve mice at 30 min post i.v. infection (**Fig.**
282 **6C**). The vaccine-activated clearance of blood-borne *K. pneumoniae* was also manifested by
283 virtual sterilization of the bloodstream in vaccinated mice at 30 min as compared with severe
284 bacteremia in naïve mice (43% of total bacteria in blood). IVM imaging revealed significantly
285 enhanced capture of circulating bacteria by KCs but not LSECs in the sinusoids of vaccinated
286 mice (**Fig. 6D** and **6I**), which is consistent with relatively low protection capacity of the WCV
287 (full mortality at higher infection dose of $10^7$ CFU, **Fig. 6A**). We further confirmed the
288 reliability of the *in vivo* immunoprotection correlates with inactivated WCV of a virulent
289 *Escherichia coli* K1 strain, a capsular serotype commonly causing human blood infection and
290 neonate meningitis[27]. The i.p. infection with a lethal dose of the same *E. coli* strain led to 100%
291 mortality in naïve mice but a complete protection in the vaccinated mice (**Fig. 6E**). In line with
292 the immunoprotection capacity, WCV immunized mice also showed rapid clearance of the
293 pathogen from the circulation (**Fig. 6F**), effective pathogen capture in the liver (**Fig. 6G**) by
294 KCs (**Fig. 6H** and **6J**), as evidenced by dominant proportion of the detectable bacteria in the
295 liver (81%) and virtual blood sterilization of each immunized mouse. It should be mentioned
296 that the KCs of *E. coli* WCV-immunized mice were much more capable of pathogen capture
297 (94 bacteria per FOV) than the counterparts of *K. pneumoniae*-WCV (13 bacteria per FOV),
298 suggesting that the former is more effective. This notion is supported by more significant
299 pathogen killing in the *E. coli* WCV-immunized mice, as indicated by more significant
300 reduction in the total bacteria in *E. coli* WCV-immunized mice (53% of the total bacteria) than
301 the *K. pneumoniae* counterparts (104% of the total bacteria). Lastly, IVM imaging did not
302 revealed any significant enhancement of pathogen capture by LSECs by either *K. pneumoniae*
303 WCV (**Fig. 6I**) or *E. coli* WCV (**Fig. 6J**), which is in sharp contrast to the dominant role of
304 LSECs in PCV13-immunized mice (**Fig. 3**). Based on the extreme importance of LSECs in
305 upgrading vaccine protection potency[20], the failure of WCV in activating pathogen capture of
306 LSECs indicated the limited efficacy of the whole cell vaccines as compared with the licensed
307 PCV13. In conclusion, these data have confirmed the reliability of our *in vivo*
308 immunoprotection correlates in quantifying the functional features and potency of vaccine-
309 activated immunity.

310 **DISCCUSSION**

311 Immunoprotection efficacy is the core function of all vaccines, regardless the natures of
312 pathogenesis and immunization. However, the current vaccine evaluation system almost
313 entirely depends on *in vitro* features of vaccine-induced responses beyond impact on host
314 disease severity and/or survival, such as antibody titer and antibody-mediated neutralization
315 and/or opsonophagocytosis[22,28,29]. The dynamics of vaccine-induced *in vivo* actions toward
316 pathogen elimination in the process of infection have remained as a "black hole". In this study,
317 we have used four different vaccines (two PCV13s and two WCVs) for three pathogens (*S.*
318 *pneumoniae*, *K. pneumoniae* and *E. coli*) to characterize an *in vivo* vaccine evaluation system,
319 based on our recent discoveries of the liver as the major immune organ to capture and kill
320 highly virulent bacteria from the blood circulation in vaccinated mice[19,20]. This system includes
321 three related vaccine-activated functions in the defense against invasive infection: pathogen
322 clearance from the bloodstream, trapping in the liver, and cellular capture by KCs and/or
323 LSECs. These correlates have thus bridged our knowledge gap between vaccine-induced
324 antibody response and immunoprotection. Despite that many effective vaccines have been
325 developed by conventional approaches, many important infectious diseases remain
326 unpreventable by vaccination. These functional features of vaccine immunity will not only
327 upgrade our understanding of vaccine biology, but may also empower future vaccine
328 development, particularly for those invasive pathogens that are able to survive in the blood
329 circulation by circumventing innate capture by Kupffer cells (encapsulated bacteria, fungi, and
330 protozoa) and LSECs (viruses).

331 We have clearly shown that the kinetics of pathogen decay in the bloodstream of
332 vaccinated mice accurately reflect the immunoprotection level of vaccines (survival rate). The
333 pneumococcal serotypes with faster clearance rates or lower $CT_{50}$ values at high infection doses
334 (serotypes 4, 5 and 6A) in PCV13-immunized mice consistently exhibited stronger immunity
335 to lethal challenge or higher $LD_{50}$ values (**Fig. 1**). Conversely, the serotypes with higher $CT_{50}$
336 counts also displayed lower $LD_{50}$ values (serotypes 1 and 3). This functional association is
337 further supported by PCV13 brand-specific correlation between blood pathogen clearance and
338 immunoprotection (**Figs. 4** and **5**). Lastly, *E. coli* WCV-immunized mice that displayed faster
339 pathogen clearance in the bloodstream than the *K. pneumoniae* counterparts also showed more
340 potent immunoprotection (**Fig. 6**). Vaccine-activated removal of invading bacteria from
341 bloodstream has been commonly used as a parameter for vaccine evaluation[20,30,31]. However,
342 to the best of our knowledge, this is the first report of demonstrating quantitative relationship
343 between vaccine-activated blood pathogen clearance and immunoprotection. An advantage of

344 this parameter is its suitability in repetitive sampling of the blood by retroorbital bleeding
345 without sacrificing the animals. Along with the dynamic detection of blood bacteria at multiple
346 time points post i.v. infection, typically within 30 min, both the clearance proportion and rate
347 of circulating bacteria can be measured (**Fig. 1**), which makes it more sensitive and quantitative.
348 Our data have shown that the vaccine-activated pathogen trapping in the liver is well
349 suited as a functional correlate for immunoprotection potency of vaccines against blood-borne
350 bacteria. Serotypes 4, 5 and 6A with the superior immunoprotection or high $LD_{50}$ values in
351 PCV13-immunzed mice displayed higher percentages of total bacteria in the liver than
352 serotypes 1 and 3, which exhibited the inferior immunoprotection and hepatic pathogen
353 trapping (**Fig. 2**). This finding was verified by functional differences of two PCV13 brands in
354 immunoprotection and hepatic trapping of five HV pneumococcal serotypes (**Figs. 4** and **5**).
355 Moreover, we have used two WCVs to confirm that vaccine-activated hepatic pathogen
356 trapping can be used to evaluate the immunoprotection potency of vaccines beyond the
357 polysaccharide conjugate vaccines. *E. coli* WCV was superior to the *K. pneumoniae* WCV in
358 both hepatic pathogen trapping and immunoprotection efficacy (**Fig. 6**). The liver has been
359 recognized as a major organ to clear blood-borne microbes for over six decades[32-37]. Our recent
360 studies have uncovered the essential role of the liver as the organ for the execution of vaccine-
361 activated immunity against blood infections of virulent bacteria[19,20], which has changed our
362 conventional view that vaccine-activated immunity eliminates blood-borne bacteria by
363 circulating phagocytes[6,38].
364 Consistent with the abovementioned causal relationship between hepatic pathogen
365 trapping and immunoprotection efficacy, this study has demonstrated that cellular pathogen
366 capture by KCs and LSECs in the liver sinusoids is a reliable and sensitive indicator of vaccine
367 immunoprotection. This relies on the state-of-art non-invasive intravital imaging technology to
368 visualize the process of pathogen capture by KCs and LSECs in the liver sinusoidal
369 vasculatures. This technique can provide multiple facets of functional information on vaccine
370 immunity: overall pathogen capture and ratio of KC- and LSEC-captured bacteria. As
371 manifested by significant difference of two WCVs in FOV value (**Fig. 6**), the vaccine activating
372 stronger pathogen capture by KCs confers more potent immunoprotection. However, as
373 indicated in our recent work[20], this study shows that LSEC-mediated pathogen capture is an
374 accurate correlate of the elite vaccine immunity. LSEC-dominant pathogen capture in the liver
375 accompanies the potent immunoprotection in PCV13-immunized mice. It is worth mentioning
376 that the levels of LSEC-captured bacteria distinguish the subtle difference of PCV13 to
377 PCV13X in immunoprotection against serotype-4 pneumococci (**Fig. 4D**), which could not be

378 differentiated by either blood pathogen clearance or hepatic pathogen trapping. In sharp
379 contrast, the mice immunized with two WCVs showed only pathogen capture by KCs and
380 relatively weaker immunoprotection efficacies. Along this line, effective activation of LSEC's
381 pathogen capture will be the direction for the development of potent vaccines for *E. coli*, *K.*
382 *pneumoniae* and other common pathogens of blood infections in humans.

383 This study has uncovered important insights into the spatial and technical venues for future
384 improvement of polysaccharide conjugate vaccines. While previous epidemiological surveys
385 have reported relatively poor protection of pneumococcal conjugate vaccines against serotype-
386 3 pneumococci in humans[24-26,39], the mechanisms behind the functional differences between
387 serotype 3 and other types have remained undefined. Our data in mouse blood infection model
388 have shown that, despite comparable levels of PCV13-induced serotype-specific IgG
389 antibodies for the five serotypes, PCV13-induced immunoprotection against serotype-3 is
390 strikingly inferior to other serotypes (e.g., $LD_{50}$ values). Accordingly, our *in vivo* vaccine
391 evaluation system reveals that PCV13 induces much poorer levels of blood pathogen clearance,
392 hepatic pathogen trapping and cellular pathogen capture in the liver. Because vaccine-induced
393 IgG antibodies, particularly IgG1 subtype, define the pathogen binding from KCs to LSECs in
394 the liver[20], our data indicate that PCV13 induces a much lower level of protective antibodies
395 to the serotype-3 capsule, which cannot be identified by measuring the total antibodies.

396 It is highly intriguing to observe substantial differences between two PCV13 brands in
397 various immunoprotective correlates. While there may be differences in manufactural
398 procedures, such as the purity of capsular polysaccharides and polysaccharide-protein
399 conjugation, it is noticeable that the two brands use different number of carrier proteins. While
400 PCV13X uses a single carrier protein for all the 13 serotypes, PCV13 contains the same carrier
401 protein as PCV13X and an additional carrier, in which 7 serotypes are conjugated to one carrier
402 while the other 6 serotypes are linked to the other carrier. The carrier protein is essential for
403 PCV to activate helper T cell to generate high-affinity antibodies and long-term memory
404 compared with polysaccharide vaccines[7]. Since both the vaccines share one carrier protein, our
405 data strongly suggest that the functional superiority of PCV13 is rooted in the extra carrier.
406 These immunological differences may be caused by excessive occupation of immunological
407 capacity by a single carrier protein in PCV13X, a phenomenon called carrier protein-induced
408 epitope suppression (CIES)[40]. The competition for helper T cells to recognize and present the
409 same carrier protein conjugated with different haptens (polysaccharides in PCV13) is the
410 molecular basis for CIES[41,42]. In other words, PCV13 may benefit from potential attenuation
411 of the CIES effect by using dividing the labor between the two carriers.

412 In summary, our *in vivo* vaccine evaluation system can not only reliably and sensitively
413 distinguish the functional features of vaccines, but also provide functional guidance to future
414 vaccine design and evaluation. The three assays of this new vaccine evaluation system can be
415 directly applicable to the evaluation and development of new vaccines for bacteria, fungi and
416 parasites that cause systemic infections, particularly the encapsulated bacteria that are
417 refractory to phagocytic clearance in the liver (e.g., *E. coli* and *K. pneumoniae*). With certain
418 technical modifications, our findings may also be used for evaluation of vaccine candidates for
419 viral pathogens that depend on viremia for dissemination and vector-borne transmission.

420 **METHOD AND MATERIAL**

421 **Bacteria strains and cultivation**

422 All the strains of *S. pneumoniae*, *E. coli* and *K. pneumoniae* used in this study are listed in
423 **Table S1**. Pneumococcal strains were cultured in Todd-Hewitt broth (THB) (Oxoid) with 0.5%
424 yeast extract or on tryptic soy agar (TSA) (BD Difco) plates with 5% defibrinated sheep blood
425 at 37℃ with 5% $CO_2$ as described[21]. *E. coli* and *K. pneumoniae* were cultured in Luria-Bertani
426 (LB) broth at 37℃ with shaking as described[19].

427

428 **Vaccines and immunoprotection**

429 PCV13 and PCV13X used in this study have been approved by the Chinese National
430 Medical Products Administration (NMPA). The two vaccines contain the same set of 13
431 capsular polysaccharide antigens or serotypes (1, 3, 4, 5, 6A, 6B, 7F, 9V, 14, 18C, 19A, 19F
432 and 23F), with an apparent difference in the carrier protein based on the information at the
433 manufacturer's websites. All the 13 CPSs are linked to a single carrier protein in PCV13X; in
434 PCV13, 7 serotypes are conjugated to the common carrier with PCV13X, whereas the other 6
435 serotypes to the second carrier.

436 C57BL/6J mice and CD1 mice were obtained from Beijing HFK Bioscience (Beijing,
437 China) and Vital River (Beijing, China), respectively, and kept in SPF facilities at Laboratory
438 Animal Resources Center of Tsinghua University. All animal experiments were conducted
439 according to animal protocols approved by the Institutional Animal Care and Use Committee
440 at Tsinghua University. Immunization with PCV13 was carried out in 5-week-old C57BL/6J
441 mice as previously described[20]. 50 μl (1/10 dose of human) of PCV13 or adjuvant (aluminum
442 phosphate) was intramuscularly (i.m.) injected. Two boost immunizations were carried out by
443 the same procedure 14 and 28 days later. Immunization with the whole cell vaccines of *E. coli*
444 and *K. pneumoniae* was carried out in 5-week-old CD1 mice as previously described[43,44].
445 Briefly, $10^8$ colony forming unit (CFU) of *E. coli* strain TH14512 (K1) or *K. pneumoniae* strain
446 TH13044 (K2) were treated with 0.5% formalin in phosphate-buffered saline (PBS) at 4°C
447 overnight, washed with PBS by centrifugation, resuspended in 475 μl PBS, and mixed with 25
448 μl of Adju-Phos® adjuvant (InvivoGen) before subcutaneous (s.c.) immunization. The same
449 procedure was repeated once 7 days later. Immune sera were collected by retro-orbital bleeding
450 2 weeks after final immunization.

451 Immunoprotection was assessed by intraperitoneal (i.p.) infection with various doses of
452 bacteria in 100 μl PBS 3 weeks post final immunization as described[20]. The animal survival

453 was observed every 12 hrs within 7 days post infection. The 50% lethal dose ($LD_{50}$) was
454 calculated by $LD_{50}$ calculator (Quest GraphTM, AAT Bioquest, Inc).
455
456 **Bacterial clearance from the bloodstream**
457 The clearance of *S. pneumoniae*, *E. coli* and *K. pneumoniae* from the bloodstream was
458 evaluated by assessing kinetics of bacteremia retro-orbital bleeding and CFU plating on TSA
459 blood plates at various time points in the first 30 min post intravenous (i.v.) inoculation of
460 bacteria in 100 µl PBS as described previously[20]. Clearance time for half of the inoculum ($CT_{50}$)
461 values were obtained as described[21].
462
463 **Bacterial trapping in the liver**
464 Bacteria trapped in the liver and other major organs (heart, kidney, lung and spleen) were
465 determined as described[20]. Briefly, bacterial burdens in the blood, heart, kidney, liver, lung and
466 spleen of each mouse were measured by CFU plating at 30 min post infection and presented as
467 CFU count for each organ. Bacteria trapped in the liver are presented as CFU count or
468 percentage of bacteria detected in the liver out of the total viable bacteria detected in the blood
469 and five major organs.
470
471 **Cellular capture of bacteria by liver immune cells**
472 Bacterial capture by KCs and LSECs was assessed by real-time intravital microscopy
473 (IVM) imaging of mouse liver with inverted confocal laser scanning microscopy as described[45].
474 The LSECs and KCs were labelled by i.v. injection of 2.5 µg AF594 anti-CD31 (BioLegend)
475 and AF647 anti-F4/80 (BioLegend) antibodies, respectively, 30 min before infection. $5 \times 10^7$
476 CFU of FITC-labeled bacteria were i.v. inoculated to track the immobile bacteria captured in
477 the liver sinusoids. FITC labeling was accomplished by incubating $10^8$ CFU of bacteria with
478 100 µl PBS containing 1 µg FITC (Sigma-Aldrich) for 30 min at room temperature in dark.
479 Images were acquired with Leica TCS SP8 confocal microscope using 10×/0.45 NA and
480 20×/0.80 NA HC PL APO objectives. The microscope was equipped with Acousto Optics
481 without filters. Fluorescence signals were detected by photomultiplier tubes and hybrid photo
482 detectors (600 × 600 pixels for time-lapse series and 1,024 × 1,024 pixels for photographs).
483 Three laser excitation wavelengths (488, 585, and 635 nm) were employed by white light laser
484 (1.5 mw, Laser kit WLL2, 470–670 nm). Real-time imaging was monitored for at least 1 min
485 post infection. More than five random fields of view (FOV) at 10 min post infection were
486 selected to quantify the bacteria captured by LSECs and KCs.

487

488 **Enzyme-linked immunosorbent assay (ELISA)**

489 CPS-specific IgG was quantified by enzyme-linked immunosorbent assay (ELISA) as
490 described[20,46]. Briefly, 96-well plates were coated with capsular polysaccharides and then
491 blocked by 5% non-fat dry milk (BD Difco). The mouse serum was serially diluted with PBS
492 and added into CPS-coated wells for two-hour incubation at 37°C. Bound antibodies were
493 detected by incubation with goat anti-mouse HRP-conjugated IgG (1:2,000, EasyBio, Beijing,
494 China) for 1 h. The optical absorbance at wavelength of 450 nm was measured after 5-minute
495 incubation of TMB substrates (TIANGEN, China) and stopped by the addition of 1 M
496 phosphoric acid.

## REFERENCES


1. Cecconi M, Evans L, Levy M, Rhodes A. Sepsis and septic shock. *Lancet* 2018; **392**(10141): 75-87.
2. Rudd KE, Johnson SC, Agesa KM, et al. Global, regional, and national sepsis incidence and mortality, 1990-2017: analysis for the Global Burden of Disease Study. *Lancet* 2020; **395**(10219): 200-11.
3. Munford RS, Suffredini AF. Sepsis, severe sepsis and septic shock. In: Bennett JE, Dolin RD, Blaser MJ, eds. Mandell, Douglas, and Bennett's Principles and Practice of Infectious Diseases. 8 ed. Philadelphia: Elsevier Health Sciences; 2014: 914-34.
4. Mayr FB, Yende S, Angus DC. Epidemiology of severe sepsis. *Virulence* 2014; **5**(1): 4-11.
5. Bogaert D, de Groot R, Hermans PWM. *Streptococcus pneumoniae* colonisation: the key to pneumococcal disease. *Lancet Infect Dis* 2004; **4**(3): 144-54.
6. Briles DE, Paton JC, Mukerji R, Swiatlo E, Crain MJ. Pneumococcal vaccines. *Microbiol Spectr* 2019; **7(6)**: GPP3-0028-2018.
7. Rappuoli R, De Gregorio E. A sweet T cell response. *Nat Med* 2011; **17**(12): 1551-2.
8. Rappuoli R. Glycoconjugate vaccines: Principles and mechanisms. *Sci Transl Med* 2018; **10**(456).
9. Wahl B, O'Brien KL, Greenbaum A, et al. Burden of *Streptococcus pneumoniae* and *Haemophilus influenzae* type b disease in children in the era of conjugate vaccines: global, regional, and national estimates for 2000-15. *Lancet Glob Health* 2018; **6**(7): e744-e57.
10. Two new pneumococcal vaccines-Prevnar 20 and Vaxneuvance. *JAMA* 2021; **326**(24): 2521-2.
11. De Gregorio E, D'Oro U, Bertholet S, Rappuoli R. Vaccines. In: Paul WE, ed. Fundamental Immunology. Philadelphia: Wolters Kluwer; 2012: 1032-68.
12. Fleck RA, Romero-Steiner S, Nahm MH. Use of HL-60 cell line to measure opsonic capacity of pneumococcal antibodies. *Clin Diagn Lab Immunol* 2005; **12**(1): 19-27.
13. Jackson LA, Gurtman A, Rice K, et al. Immunogenicity and safety of a 13-valent pneumococcal conjugate vaccine in adults 70 years of age and older previously vaccinated with 23-valent pneumococcal polysaccharide vaccine. *Vaccine* 2013; **31**(35): 3585-93.
14. Kubes P, Jenne C. Immune responses in the liver. *Annu Rev Immunol* 2018; **36**: 247-77.
15. Racanelli V, Rehermann B. The liver as an immunological organ. *Hepatology* 2006; **43**(2 Suppl 1): S54-62.
16. Bilzer M, Roggel F, Gerbes AL. Role of Kupffer cells in host defense and liver disease. *Liver Int* 2006; **26**(10): 1175-86.
17. Krenkel O, Tacke F. Liver macrophages in tissue homeostasis and disease. *Nat Rev Immunol* 2017; **17**(5): 306-21.
18. Sorensen KK, Simon-Santamaria J, McCuskey RS, Smedsrod B. Liver sinusoidal endothelial cells. *Compr Physiol* 2015; **5**(4): 1751-74.
19. Huang X, Li X, An H, et al. Capsule type defines the capability of *Klebsiella pneumoniae* in evading Kupffer cell capture in the liver. *PLoS Pathog* 2022; **18**(8): e1010693.
20. Wang J, An H, Ding M, et al. Potent bacterial vaccines require FcγRIIB-mediated pathogen capture by liver sinusoidal endothelium. *bioRxiv* 2022; doi: 2022.07.19.500551.
21. An H, Qian C, Huang Y, et al. Functional vulnerability of liver macrophages to capsules defines virulence of blood-borne bacteria. *J Exp Med* 2022; **219**(4): e20212032.
22. LaFon DC, Nahm MH. Measuring immune responses to pneumococcal vaccines. *J Immunol Methods* 2018; **461**: 37-43.
23. Recommendations to assure the quality, safety and efficacy of pneumococcal conjugate vaccines, Annex 3, TRS No 977. 2013.
24. Slotved HC, Dalby T, Harboe ZB, et al. The incidence of invasive pneumococcal serotype 3 disease in the Danish population is not reduced by PCV-13 vaccination. *Heliyon* 2016; **2**(11):

547 e00198.
548 25. Lapidot R, Shea KM, Yildirim I, Cabral HJ, Pelton SI, Department Of Public Health TM.
549 Characteristics of serotype 3 invasive pneumococcal disease before and after universal
550 childhood immunization with PCV13 in Massachusetts. *Pathogens* 2020; **9**(5).
551 26. Menzies R, Stein AN, Booy R, Van Buynder PG, Litt J, Cripps AW. The impact of the
552 changing pneumococcal national immunisation program among older Australians. *Vaccine*
553 2021; **39**(4): 720-8.
554 27. Rhee C, Wang R, Zhang Z, et al. Epidemiology of hospital-onset versus community-onset
555 sepsis in U.S. hospitals and association with mortality: a retrospective analysis using electronic
556 clinical data. *Crit Care Med* 2019; **47**(9): 1169-76.
557 28. Paschall AV, Middleton DR, Avci FY. Opsonophagocytic killing assay to assess
558 immunological responses against bacterial pathogens. *J Vis Exp* 2019; (146).
559 29. Plotkin SA. Correlates of protection induced by vaccination. *Clin Vaccine Immunol* 2010;
560 **17**(7): 1055-65.
561 30. Brown EJ, Hosea SW, Frank MM. The role of antibody and complement in the
562 reticuloendothelial clearance of pneumococci from the bloodstream. *Rev Infect Dis* 1983; **5**
563 **Suppl 4**: S797-805.
564 31. Li Y, Hill A, Beitelshees M, et al. Directed vaccination against pneumococcal disease. *Proc*
565 *Natl Acad Sci U S A* 2016; **113**(25): 6898-903.
566 32. Martin SP, Kerby GP, Holland BC. A method for measuring removal of bacteria from the
567 blood by the various organs of the intact animal. *Proc Soc Exp Biol Med* 1949; **72**(1): 63-8.
568 33. Rogers DE. Studies on bacteriemia. I. Mechanisms relating to the persistence of
569 bacteriemia in rabbits following the intravenous injection of *Staphylococci*. *J Exp Med* 1956;
570 **103**(6): 713-42.
571 34. Benacerraf B, Sebestyen MM, Schlossman S. A quantitative study of the kinetics of blood
572 clearance of $P^{32}$-labelled *Escherichia coli* and *Staphylococci* by the reticuloendothelial system.
573 *J Exp Med* 1959; **110**(1): 27-48.
574 35. Mackaness GB. Cellular resistance to infection. *J Exp Med* 1962; **116**: 381-406.
575 36. Brown EJ, Hosea SW, Frank MM. The role of complement in the localization of
576 pneumococci in the splanchnic reticuloendothelial system during experimental bacteremia. *J*
577 *Immunol* 1981; **126**(6): 2230-5.
578 37. Gregory SH, Sagnimeni AJ, Wing EJ. Bacteria in the bloodstream are trapped in the liver
579 and killed by immigrating neutrophils. *J Immunol* 1996; **157**(6): 2514-20.
580 38. Nahm MH, Katz J. Immunity to extracellular bacteria. In: E.P. W, ed. Fundamental
581 Immunology. 6th ed. Philadephia: Lippincott-Raven Publishers; 2012: 1001-15.
582 39. Andrews NJ, Waight PA, Burbidge P, et al. Serotype-specific effectiveness and correlates
583 of protection for the 13-valent pneumococcal conjugate vaccine: a postlicensure indirect cohort
584 study. *Lancet Infect Dis* 2014; **14**(9): 839-46.
585 40. Pobre K, Tashani M, Ridda I, Rashid H, Wong M, Booy R. Carrier priming or suppression:
586 understanding carrier priming enhancement of anti-polysaccharide antibody response to
587 conjugate vaccines. *Vaccine* 2014; **32**(13): 1423-30.
588 41. Herzenberg LA, Tokuhisa T. Epitope-specific regulation. I. Carrier-specific induction of
589 suppression for IgG anti-hapten antibody responses. *J Exp Med* 1982; **155**(6): 1730-40.
590 42. Dagan R, Goldblatt D, Maleckar JR, Yaich M, Eskola J. Reduction of antibody response to
591 an 11-valent pneumococcal vaccine coadministered with a vaccine containing acellular
592 pertussis components. *Infect Immun* 2004; **72**(9): 5383-91.
593 43. Serushago BA, Mitsuyama M, Handa T, Koga T, Nomoto K. Role of antibodies against
594 outer-membrane proteins in murine resistance to infection with encapsulated *Klebsiella*
595 *pneumoniae*. *J Gen Microbiol* 1989; **135**(8): 2259-68.
596 44. Gohar A, Abdeltawab NF, Fahmy A, Amin MA. Development of safe, effective and

597 immunogenic vaccine candidate for diarrheagenic *Escherichia coli* main pathotypes in a mouse
598 model. *BMC Res Notes* 2016; **9**: 80.
599 45. Wang J, Kubes P. A reservoir of mature cavity macrophages that can rapidly invade visceral
600 organs to affect tissue repair. *Cell* 2016; **165**(3): 668-78.
601 46. Wang Y, Wen Z, Pan X, Briles DE, He Y, Zhang JR. Novel immunoprotective proteins of
602 *Streptococcus pneumoniae* identified by opsonophagocytosis killing screen. *Infect Immun* 2018;
603 **86**(9) e00423-18.
604
605

**Acknowledgments:** We thank Tsinghua research platforms for assistance in animal experimentation (Laboratory Animal Research Center) and IVM imaging (Center for Cell Biology).

**Funding:** This work was supported by grants from National Natural Science Foundation of China 31820103001, 31530082, 81671972, 31728002 (J.-R.Z.) and 3210010245 (J.W.); China Postdoctoral Science Foundation 2020M680518 (J.W.); Tsinghua-Peking Joint Center for Life Sciences Postdoctoral Foundation (J.W.).

**Author contributions:**

Conceptualization: X.T., J.W., J.-R.Z.;

Experimentation: X.T., J.W., H.C., M.D., Q.J., J.-R.Z.;

Methodology: X.T., J.W., H.C., M.D., Q.J.;

Investigation: J X.T., J.W., J.-R.Z.;

Funding: J.W., J.-R.Z.;

Project administration: J.W., J.-R.Z.;

Supervision: X.T., J.W., J.-R.Z.;

Writing original draft: X.T., J.W., J.-R.Z.;

**Competing interests:**

Patent applications have been filed on the basis of this work.

**Data and materials availability:**

All data are available in the main text or the supplementary materials.

627

# FIGURES AND LEGENDS

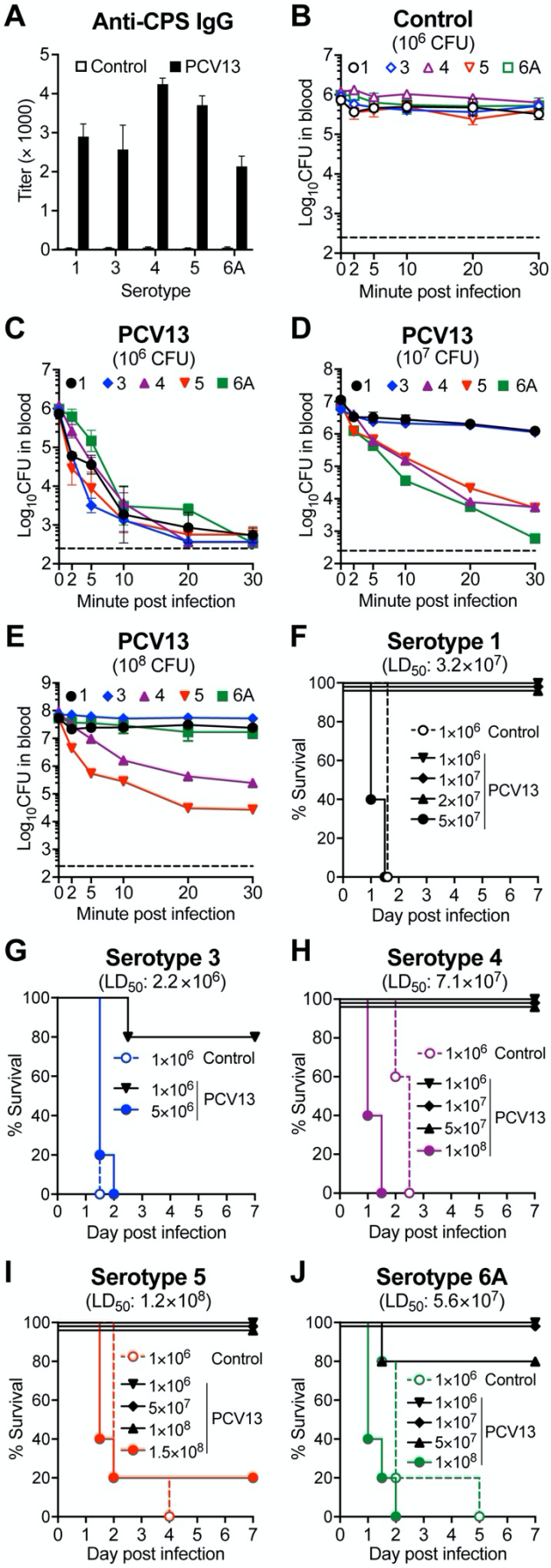


628

629 **Figure 1. Vaccine-activated pathogen clearance from the circulation in PCV13-imminzed**
630 **mice**.
631 **(A)** CPS-specific IgG titers of serotype 1, 3, 4, 5, 6A in sera of adjuvant-treated (control) and
632 PCV13-immunized mice as detected by ELISA. n = 3-5.
633 **(B)** Bacteremia levels of adjuvant-treated mice i.v. infected with $10^6$ CFU of serotype-1, -3, -
634 4, -5, -6A pneumococci in the first 30 min. n = 3.
635 **(C-E)** Bacteremia level of PCV13-immunized mice i.v. infected with $10^6$ (**C**), $10^7$ (**D**) or $10^8$
636 (**E**) CFU of serotype-1, -3, -4, -5, -6A pneumococci in the first 30 min. n = 3.
637 **(F-J)** Survival rate of adjuvant-treated and PCV13-immunized mice i.p. infection with various
638 doses of serotype-1 (**F**), -3 (**G**), -4 (**H**), -5 (**I**) or -6A (**J**) pneumococci. $LD_{50}$ is presented at the
639 top. n = 5.
640 Data presented as the mean values ± standard error of mean (SEM). Dotted line in (B-E)
641 indicates the limit of detection.
642

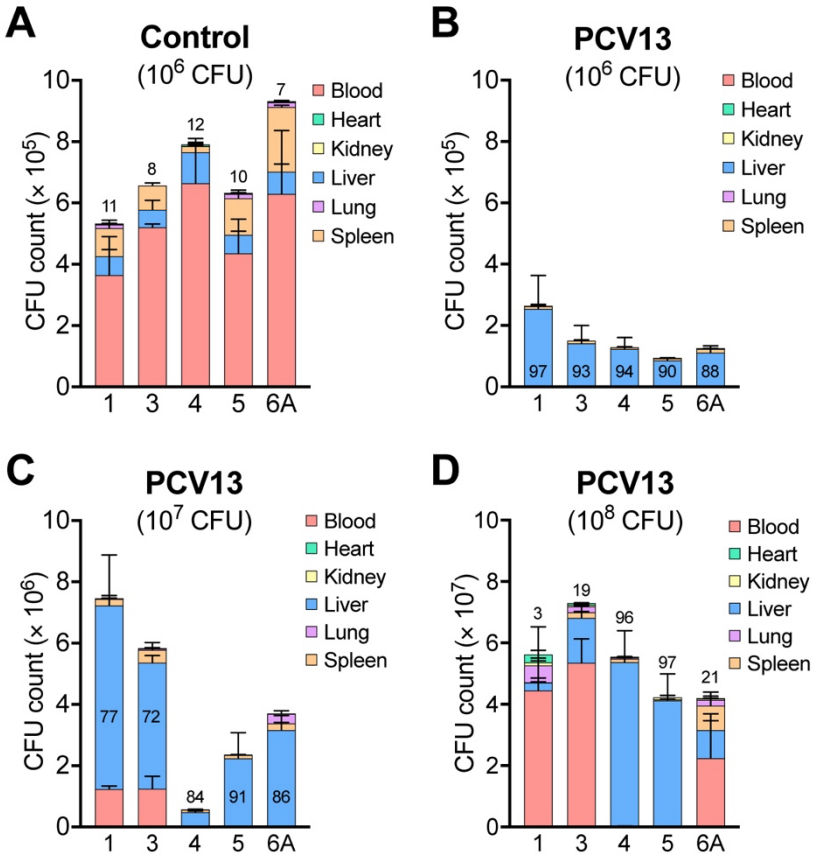


**Figure 2. Vaccine-activated hepatic trapping of blood-borne pneumococci in PCV13-immunized mice.**

**(A)** Proportional bacterial burden in the blood and each of the five major organs of adjuvant-treated mice at 30 min post i.v. infection with $10^6$ CFU of serotype-1, -3, -4, -5 and -6A pneumococci. Relative proportion of hepatic bacteria is presented in or at the top of each bar as a percentage of total bacteria detected in each mouse. n = 3.

(**B-D**) Proportional bacterial burden in the blood and five major organs of PCV13-immunized mice at 30 min post i.v. infection with $10^6$ (**B**), $10^7$ (**C**) or $10^8$ (**D**) CFU of serotype-1, -3, -4, -5 and -6A pneumococci. Relative proportion of hepatic bacteria is presented in each bar as in (A).

Data presented as the mean values ± standard error of mean (SEM).

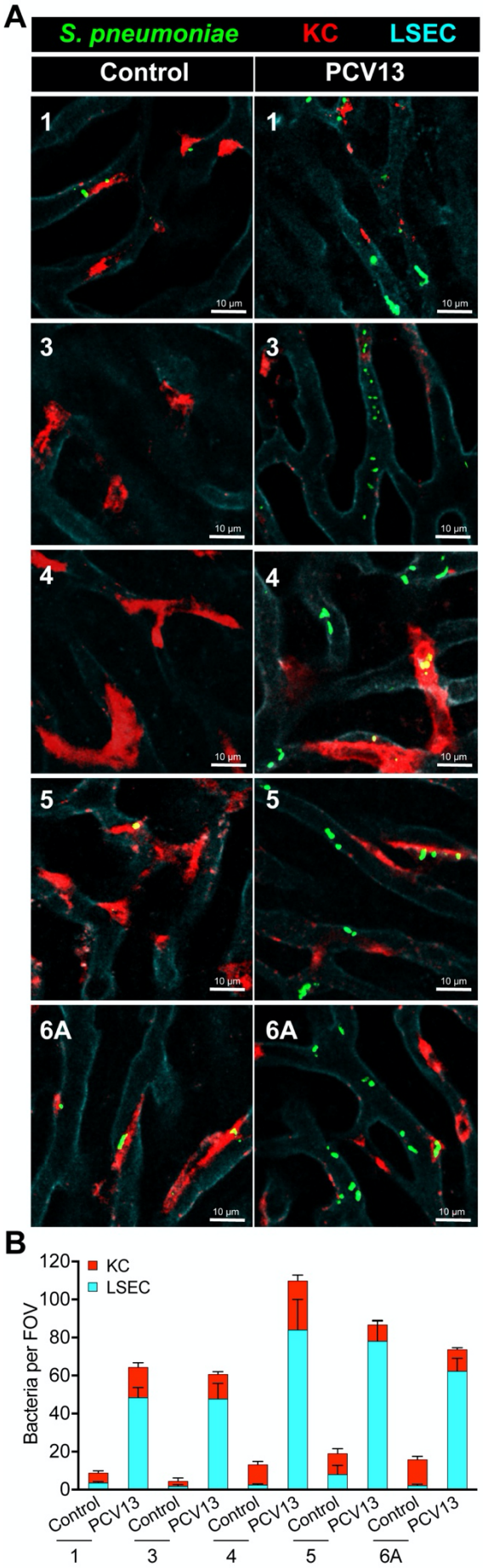
A
S. pneumoniae
KC
LSEC
Control
PCV13
1
3
4
5
6A
10 µm
B
KC
LSEC
Bacteria per FOV
120
100
80
60
40
20
0
Control
PCV13
1
3
4
5
6A

655

656 **Figure 3. Vaccine-activated pathogen capture by LSECs and KCs in PCV13-immunized**
657 **mice.**
658 **(A)** Representative IVM images of pneumococci (green), Kupffer cells (KCs, red) and liver
659 sinusoid endothelial cells (LSECs, cyan) in the liver sinusoids of adjuvant-treated (control, left
660 panel) or PCV13-immunized (right panel) mice 10 min after i.v. infection with $5 \times 10^7$ CFU of
661 serotype-1, -3, -4, -5 and -6A pneumococci. n = 2. The process of bacterial capture is
662 demonstrated in Movies 1-5.
663 **(B)** Quantitation of bacteria immobilized on LSECs and KCs of adjuvant-treated (control) or
664 PCV13-immunized mice in at least five random fields of view (FOV).
665 Data presented as the mean values ± standard error of mean (SEM).

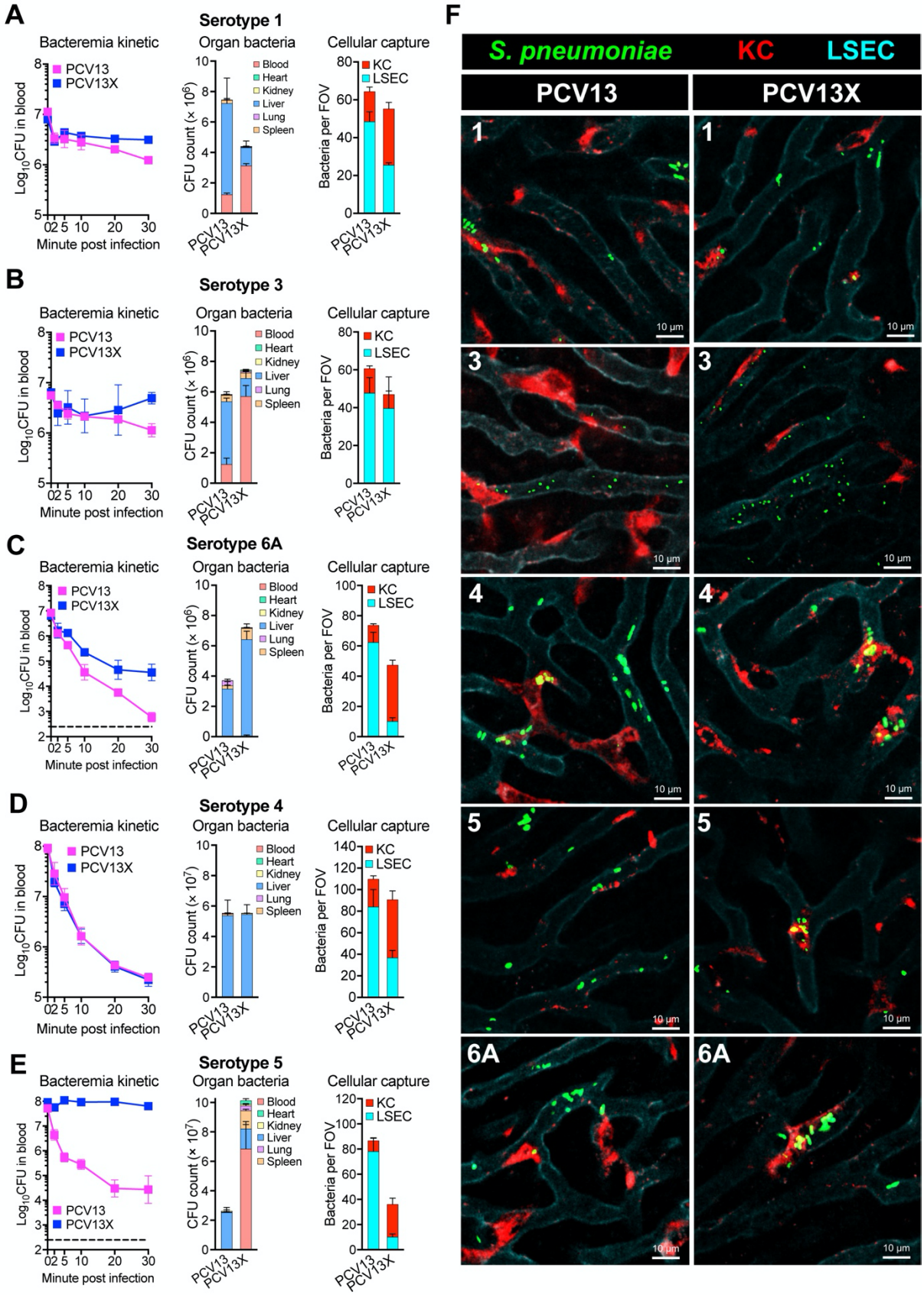


**Figure 4. Brand-specific functional variations of PCV13 revealed by the *in vivo* immunoprotection correlates.**

669 **(A-E)** Bacteremia in the first 30 min (left panel), bacterial burden in the blood and major organs
670 at 30 min (middle panel), and bacterial capture by LSECs and KCs (right panel) in PCV13- or
671 PCV13X-immunized mice post i.v. infection with serotype-1 (**A**), -3 (**B**), -6A (**C**), -4 (**D**) and
672 -5 (**E**) pneumococci. Relative proportion of hepatic bacteria is indicated in or above each bar
673 as in Fig. 2A. The data for the first two panels for each serotype were derived from the same
674 experiment with the following infection dose: $10^7$ CFU for serotypes 1, 3 and 6A; $10^8$ CFU for
675 serotypes 4 and 5. Bacterial capture (n = 2) was quantitated by IVM imaging as in Fig. 3B.
676 **(F)** Representative IVM images of the liver sinusoids in PCV13- (left panel) or PCV13X-
677 immunized (right panel) mice 10 min after i.v. infection with $5 \times 10^7$ CFU of serotype-1, -3, -
678 4, -5 and -6A pneumococci as in Fig. 3A. The process of bacterial capture is demonstrated in
679 Movie 6 (serotype 1), Movie 7 (serotype 3), Movie 8 (serotype 6A), Movie 9 (serotype 4), and
680 Movie 10 (serotype 5).
681

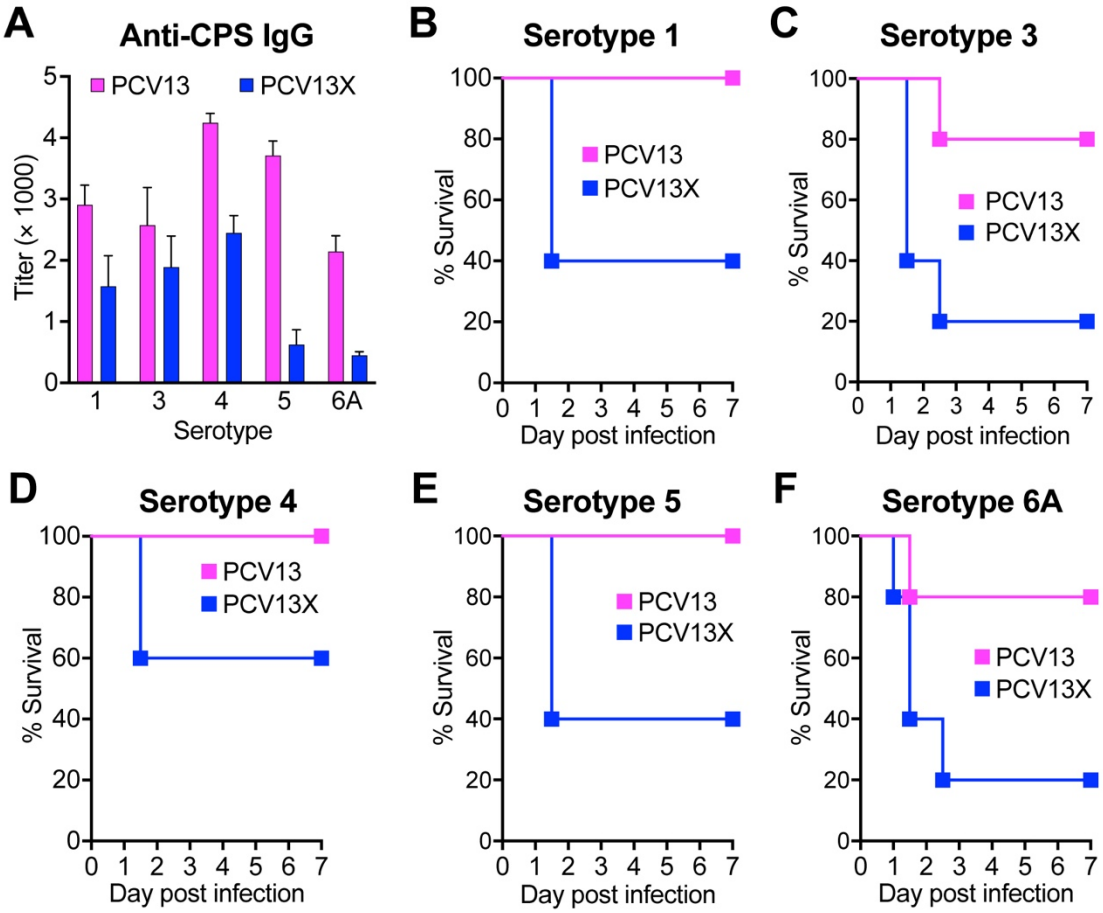


682

683 **Figure 5. Antibody titer and immunoprotection of efficacy in PCV13- and PCV13X-**
684 **immunized mice.**

685 **(A)** CPS-specific IgG titers of serotype 1, 3, 4, 5 and 6A in sera of PCV13- or PCV13X-
686 immunized mice. n = 3-5.

687 **(B-F)** The survival of PCV13- or PCV13X-immunized mice post i.p. infection with $2 \times 10^7$
688 CFU serotype-1 (**B**), $1 \times 10^6$ CFU serotype-3 (**C**), $5 \times 10^7$ CFU serotype-4 (**D**), $1 \times 10^8$ CFU
689 serotype-5 (**E**) or $5 \times 10^7$ CFU serotype-6A (**F**) pneumococci. n = 5.

690 Data presented as the mean values ± standard error of mean (SEM).

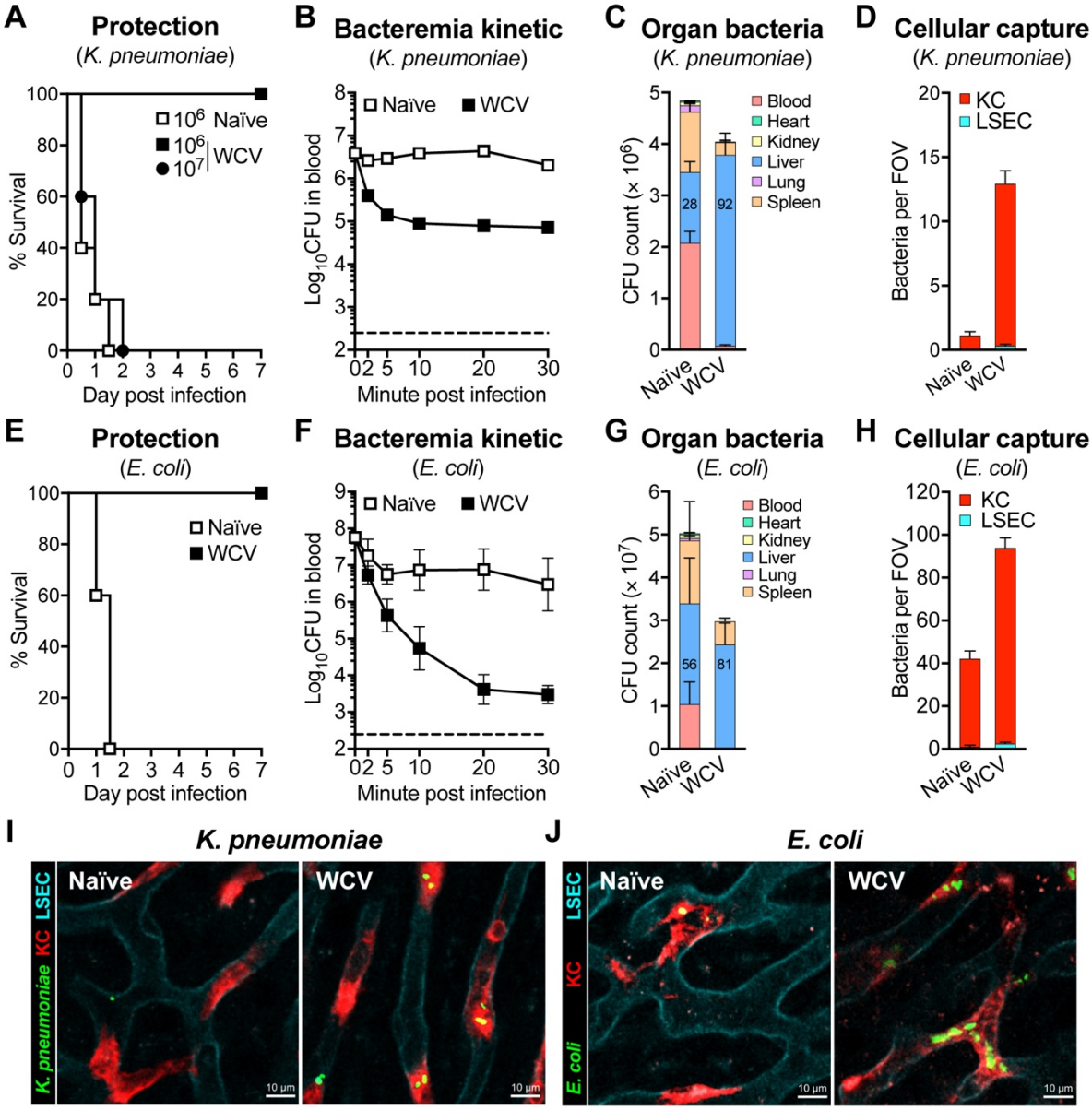


**Figure 6. Vaccine-activated pathogen clearance, trapping in the liver and capture by Kupffer cells in whole cell vaccine (WCV)-immunized mice.**

**(A-D)** Functional features of *K. pneumoniae* WCV. Host survival (**A**), bacteremia in the first 30 min (**B**), bacterial burden in blood and major organs at 30 min (**C**), and bacterial capture by LSECs and KCs (**D**) post infection of *K. pneumoniae* strain TH13044 (serotype K2) in naïve or WCV-immunized mice. Infections were performed with the following doses and routes: $10^6$ or $10^7$ CFU (i.p.) for (A), $5 \times 10^6$ CFU (i.v.) for (B-C), $5 \times 10^7$ CFU (i.v.) for (D). n = 5 for (A), 3 for (B-C), and 2 for (D).

**(E-H)** Functional features of *K. pneumoniae* WCV. Host survival (**E**), bacteremia (**F**), bacterial burden in blood and major organs (**G**), and bacterial capture (**H**) post infection of *E. coli* strain TH14512 (serotype K1) in naïve or WCV-immunized mice. Infections were performed with

703 the following doses and routes: $5 \times 10^7$ CFU (i.p.) for (E), $10^8$ CFU (i.v.) for (F-G), $5 \times 10^7$
704 CFU (i.v.) for (H). n = 5 for (E), 3 for (F-G), and 2 for (H).
705 **(I-J)** Representative IVM images of the liver sinusoids in naive (left panel) or WCV-
706 immunized (right panel) mice 10 min after i.v. infection with $5 \times 10^7$ CFU of *K. pneumoniae*
707 **(I)** and *E. coli* **(J)** as in Fig. 3A. The process of bacterial capture is demonstrated in Movies 11-
708 12.
709 Data presented as the mean values ± standard error of mean (SEM).
710

711 **SUPLMENATRY MATERIALS**

712 **Table S1. Bacterial strains used in this study**

| Strain ID | Species | Serotype | Source | Region | Reference |
|---|---|---|---|---|---|
| TH2866 | *S. pneumoniae* | 1 | Blood | China | [21] |
| TH865 | *S. pneumoniae* | 3 | Cerebrospinal Fluid | USA | [21] |
| TIGR4 | *S. pneumoniae* | 4 | Blood | Norway | [21] |
| TH2940 | *S. pneumoniae* | 5 | Blood | China | [21] |
| TH870 | *S. pneumoniae* | 6A | Blood | USA | [21] |
| TH13044 | *K. pneumoniae* | K2 | Blood | China | [19] |
| TH14512 | *E. coli* | K1 | Blood | China | [21] |

713

714 **Movie 1-5. PCV13-elicited pneumococcal capture of high-virulence serotypes in liver**
715 **sinusoid.** Capture of i.v. inoculated serotype-1 (Movie 1), -3 (Movie 2), -4 (Movie 3), -5
716 (Movie 4) and -6A (Movie 5) pneumococci ($5 \times 10^7$ CFU, FITC-labelled, green) from the
717 bloodstream by liver sinusoid endothelial cells (LSECs, cyan) and resident macrophage
718 Kupffer cells (KCs, red) in adjuvant-treated (control) or PCV13-immunized mice. Real-time
719 imaging was visualized for at least 1 minute by intravital microscopy immediately post
720 infection. The playback rate is eight frames per second. The quantitative data were shown in
721 Fig. 3B; selected images in Fig. 3A.

722

723 **Movie 6-10. More efficient pneumococcal capture in liver sinusoids elicited by PCV13**
724 **than PCV13X.** $5 \times 10^7$ CFU of FITC-labelled serotype-1 (Movie 6), -3 (Movie 7), -6A (Movie
725 8), -4 (Movie 9) and -5 (Movie 10) pneumococci in PCV13-or PCV13X-immunized mice were
726 visualized as in Movie 1. The quantitative data were shown in Figs. 4A-E; selected images in
727 Fig. 4F.

728

729 **Movie 11-12. Whole cell vaccine induced capture of *K. pneumoniae* and *E. coli* by KCs**. 5
730 $\times 10^7$ CFU of FITC-labelled *K. pneumoniae* strain TH13044 (Movie 11) and *E. coli* strain
731 TH14512 (Movie 12) in naive or WCV-immunized mice were visualized as in Movie 1. The
732 quantitative data were shown in Fig. 6D and 6H; selected images in Figs. 6I-J.

733